

RESEARCH LETTER

10.1029/2017GL076457

Key Points:

- Mean methane flux (F_{CH_4}) from a tropical peat forest during the early wet season, $0.024 \text{ g C-CH}_4/\text{m}^2/\text{d}^{-1}$, was similar to tropical rice and boreal fen ecosystems
- Models explained only 11% of the variance of F_{CH_4} at daily time scales across the entire measurement period
- Whole-year whole-ecosystem F_{CH_4} measurements across multiple tropical ecosystems will help to constrain their role in the global methane budget

Supporting Information:

- Supporting Information S1

Correspondence to:

A. C. I. Tang,
atchiemac@gmail.com

Citation:

Tang, A. C. I., Stoy, P. C., Hirata, R., Musin, K. K., Aeries, E. B., Wenceslaus, J., & Melling, L. (2018). Eddy covariance measurements of methane flux at a tropical peat forest in Sarawak, Malaysian Borneo. *Geophysical Research Letters*, 45, 4390–4399. <https://doi.org/10.1029/2017GL076457>

Received 17 NOV 2017

Accepted 7 APR 2018

Accepted article online 19 APR 2018

Published online 5 MAY 2018

©2018. The Authors.

This is an open access article under the terms of the Creative Commons Attribution-NonCommercial-NoDerivs License, which permits use and distribution in any medium, provided the original work is properly cited, the use is non-commercial and no modifications or adaptations are made.

Eddy Covariance Measurements of Methane Flux at a Tropical Peat Forest in Sarawak, Malaysian Borneo

Angela C. I. Tang^{1,2} , Paul C. Stoy¹ , Ryuichi Hirata³, Kevin K. Musin², Edward B. Aeries², Joseph Wenceslaus², and Lulie Melling² 

¹Department of Land Resources and Environmental Sciences, Montana State University, Bozeman, MT, USA, ²Sarawak Tropical Peat Research Institute, Kuching-Kota Samarahan Expressway, Kota Samarahan, Malaysia, ³Center for Global Environmental Research, National Institute for Environmental Studies, Tsukuba, Japan

Abstract Tropical biogenic sources are a likely cause of the recent increase in global atmospheric methane concentration. To improve our understanding of tropical methane sources, we used the eddy covariance technique to measure CH_4 flux (F_{CH_4}) between a tropical peat forest ecosystem and the atmosphere in Malaysian Borneo over a 2-month period during the wet season. Mean daily F_{CH_4} during the measurement period, on the order of $0.024 \text{ g C-CH}_4/\text{m}^2 \cdot \text{day}^{-1}$, was similar to eddy covariance F_{CH_4} measurements from tropical rice agroecosystems and boreal fen ecosystems. A linear modeling analysis demonstrated that air temperature (T_{air}) was critical for modeling F_{CH_4} before the water table breached the surface and that water table alone explained some 20% of observed F_{CH_4} variability once standing water emerged. Future research should measure F_{CH_4} on an annual basis from multiple tropical ecosystems to better constrain tropical biogenic methane sources.

Plain Language Summary Methane (CH_4) is the third most potent greenhouse gas, and its reduction is seen as an effective method for meeting global temperature targets, but the global growth rate of atmospheric CH_4 concentration has risen to 10.3 ± 2.1 ppb/year from 2014 to 2016 after a period of relative stagnation from 2000 to 2006. Recent research has pointed to tropical biogenic sources as a likely cause. However, no studies to our knowledge have measured whole-ecosystem CH_4 flux (F_{CH_4}) from a tropical peat forested wetland to date despite the importance of tropical wetlands to global CH_4 budget. To improve our understanding of tropical methane sources, we measured F_{CH_4} between a tropical peat forest ecosystem in Malaysian Borneo and the atmosphere over a 2-month period during the dry to wet season transition. Mean daily F_{CH_4} during the measurement period, on the order of $0.024 \text{ g C-CH}_4/\text{m}^2 \cdot \text{day}^{-1}$, are similar to eddy covariance measurements from tropical rice agroecosystems and boreal fen ecosystems. A linear modeling analysis demonstrated the important role of air temperature (T_{air}) during unsaturated conditions and water table during saturated conditions and further emphasizes the critical role of simulating temperature and water table accurately for accurate modeled ecosystem scale F_{CH_4} estimates.

1. Introduction

The contribution of methane (CH_4) to global radiative forcing is only exceeded by water vapor (H_2O) and carbon dioxide (CO_2), and CH_4 absorbs 28 times more heat in the atmosphere than an equivalent amount of CO_2 over the course of a century (Myhre et al., 2013). Due to its relatively high potency and short atmospheric life span of about 10 years, a reduction in CH_4 emissions is seen as an effective approach for mitigating climate change (Shindell et al., 2012). Global atmospheric CH_4 concentrations, however, are on the rise, and its growth rate increased from 0.5 ± 3.1 ppb/year from 2000 to 2006 to 7.1 ± 2.6 ppb/year from 2007 to 2013 with a further increase to 10.3 ± 2.1 ppb/year from 2014 to 2016 (Dlugokencky, 2017) for reasons that are still poorly understood.

Previous studies have come to different conclusions regarding the drivers of the atmospheric CH_4 growth rate over the past decades, making it difficult for national or regional policy makers to effectively implement strategies to control the sources of CH_4 emissions. Explanations for recent changes in atmospheric CH_4 growth rate include changes in atmospheric sinks from the hydroxyl radical (Turner et al., 2017), changes in fossil fuel emissions (Aydin et al., 2011; Hausmann et al., 2016; Helmig et al., 2016; Rice et al., 2016;

Simpson et al., 2012) and changes in biogenic sources (Schaefer et al., 2016) including agricultural management (Kai et al., 2011; Levin et al., 2012). A number of lines of evidence emphasize the critical role of biogenic sources to the recent CH₄ growth rate (Worden et al., 2017) especially tropical agricultural and natural wetland ecosystems (Bousquet et al., 2011; Pandey et al., 2017; Pison et al., 2013; Nisbet et al., 2016; Saunio, Jackson, et al., 2016; Schwietzke et al., 2016).

Nearly two thirds of the global methane emissions of approximately 550 Tg CH₄/year are thought to originate from tropical sources (Denman et al., 2007; Kirschke et al., 2013; Saunio, Bousquet, et al., 2016) and nearly one third from natural wetlands (Kirschke et al., 2013; Saunio, Bousquet, et al., 2016). At the regional scale, Southeast Asia is estimated to emit 73 Tg CH₄/year, dominated by wetland emissions (~37%) and agriculture and waste emissions (~33%; Saunio, Bousquet, et al., 2016). Wetland emissions remain the largest uncertainty in the global methane budget (Kirschke et al., 2013; Saunio, Bousquet, et al., 2016), owing in part to a lack of observations. No studies to our knowledge have measured whole-ecosystem CH₄ flux (F_{CH_4}) from a tropical peat forested wetland to date despite the importance of tropical wetlands to global CH₄ efflux and recent studies demonstrating that the areal extent of tropical peat forests is greater than previously thought (Dargie et al., 2017).

Here we measure F_{CH_4} between a tropical peat forest in Sarawak, Malaysian Borneo, and the atmosphere during the wet season using the eddy covariance technique. We choose the eddy covariance system to make whole-ecosystem F_{CH_4} measurements given recent findings that CH₄ transport through tree stems may be an important pathway that cannot be accounted for using soil chamber methods (Pitz & Megonigal, 2017) and is a critical contribution of ecosystem-scale methane flux in tropical peatlands (Pangala et al., 2013, 2017). Eddy covariance can also measure aerobic CH₄ emissions from vegetated canopies via ultraviolet irradiation of pectin (Keppler et al., 2006), noting that recent studies demonstrate that this is likely to be a minor source of atmospheric methane (McLeod et al., 2008), on the order of 0.2–1.0 Tg CH₄/year (Bloom et al., 2010). We place particular emphasis on understanding the mechanisms that control ecosystem F_{CH_4} at the ecosystem scale and discuss our F_{CH_4} measurements in the context of similar measurements from other global ecosystems.

2. Materials and Methods

2.1. Study Ecosystem and Micrometeorological Measurements

The study ecosystem is a tropical peat swamp forest in Maludam National Park in the Betong Division of Sarawak, Malaysia. The terrain is relatively flat and homogenous across the site. Dominant vegetation in the overstory includes *Shorea albida*, *Gonystylus bancanus*, and *Stemonurus* spp. (Anderson, 1972) with an average canopy height of 35 m. The peat thickness is ~8 m in the vicinity of the tower located at 1°27'13"N, 111°8'58"E. A standard suite of micrometeorological measurements including rainfall (P), wind speed, air temperature (T_{air}), relative humidity (RH), and thereby the vapor pressure deficit, volumetric soil water content (SWC), soil temperature (T_{soil}), incident photosynthetically photon flux densities (PPFDs), net radiation (R_n) and global radiation (R_g), and water table (WT) height was made and recorded at half-hourly intervals as described in the supporting information. We compare micrometeorological measurements from the 2-month period when F_{CH_4} was measured against 4 years of available micrometeorological observations to emphasize conditions in which our observations were made versus a more complete range of micrometeorological variability at the study site.

2.2. Eddy Covariance Measurements

Eddy covariance measurements of methane flux (F_{CH_4}) and carbon dioxide flux (F_{CO_2}) were made from 1 November to 31 December 2013 at 41 m using an open-path LI-7700 infrared gas analyzer for CH₄ and LI-7500 infrared gas analyzer for CO₂ (LiCor, Lincoln, NE, United States), both coupled to a CSAT3 three-dimensional sonic anemometer (Campbell Scientific, Logan, UT, United States). Postprocessing calculations were performed using EddyPro software (LiCor). Double rotation was performed to align the x axis of the sonic anemometer with the mean flow, and the Webb-Pearman-Leuning (WPL) correction (Webb et al., 1980) was applied to compensate the density fluctuation effect and spectroscopic effect on measured CH₄ and CO₂. Fluxes were corrected for frequency response losses (Massman, 2000), and the time lag between wind measurements and CH₄ and CO₂ concentration measurements was compensated for each averaging period.

We select F_{CH_4} observations with a LI-7700 relative signal strength indicator (RSSI) greater than 10% following the recommendations of McDermitt et al. (2011) and Chu et al. (2014) and explore the sensitivity of this threshold in the supporting information (see Text S2 and Figure S1) given the frequency of dew formation events that reduce the RSSI in tropical forest ecosystems with characteristically high dew points. To remove measurements of both F_{CH_4} and F_{CO_2} made under conditions of insufficient turbulence, we used the atmospheric stability threshold after Novick et al. (2004), which requires near-neutral atmospheric stability ($|\zeta| < 0.1$) for nighttime (PPFD $< 5 \mu\text{mol}\cdot\text{m}^{-2}\cdot\text{s}^{-1}$) data acceptance given recent findings that common friction velocity (u^*) filters do not adequately remove periods of insufficient turbulence from forested canopies (Hayek et al., 2018; Jocher et al., 2017). Atmospheric stability is defined as $\zeta = (z - d)/L$, where z is the measurement height of the sonic anemometer, d is the zero-plane displacement height taken to be 10% of mean canopy height following Campbell and Norman (2012), and L is the Obukhov length. In addition to the atmospheric stability filter, a friction velocity (u^*) threshold value of 0.1 m/s was included to further ensure that F_{CH_4} and F_{CO_2} observations with insufficient turbulence were excluded from the analysis following Novick et al. (2004).

We present F_{CH_4} data from the top of the canopy as within-canopy CH_4 concentration measurements were not made to calculate a storage flux, which is negligible at diurnal time scales. We test the sensitivity of this assumption for whole-ecosystem fluxes by approximating storage fluxes using the one point time derivative (Gu et al., 2012) in the supporting information (see Text S3 and Figure S2). A LI-820 closed-path CO_2 analyzer (LI-COR) was deployed to measure the vertical profile of the CO_2 mixing ratio (c) at six levels within and above the canopy at 0.5, 1, 3, 11, 21, and 41 m. Air was drawn from each inlet at the tower, and the sampling path was rotated every minute. Thus, the measurement for six levels took 6 min and the concentration was averaged over 30 min. The net ecosystem exchange of CO_2 (NEE) was calculated as the sum of F_{CO_2} and the storage flux (F_s). The F_s was inferred from c profiles following Aubinet et al. (2001):

$$F_s = \frac{P_a}{RT_a} \int_0^h \frac{\partial c(z)}{\partial t} dz, \quad (1)$$

where P_a , R , and T_a are, respectively, the ambient pressure (N/m), molar constant ($\text{N}\cdot\text{m}\cdot\text{mol}^{-1}\cdot\text{K}^{-1}$), and air temperature (K); h , $c(z)$, t , and z represent the F_{CO_2} measurements (m), time (s), and vertical distance from ground surface (m), respectively.

2.3. Gap Filling of Flux Data

Continuous time series of scalar fluxes are not possible with eddy covariance systems due to periods of insufficient turbulence and disturbances like rain events that impede sonic anemometers and open path infrared gas analyzers. To obtain continuous time series to create daily and monthly sums of F_{CH_4} , we used the marginal distribution sampling gap filling algorithm (Reichstein et al., 2005) as implemented in the REdDyProc package (Reichstein & Moffat, 2014). The routine adopts the look-up table approach where a missing value is replaced by the mean value under similar meteorological conditions (R_g , vapor pressure deficit, RH, T_{air} , and T_s), and the mean diurnal course method is used if the value could not be filled using look-up table approach. We use this data-driven approach to minimize assumptions that model-based gap filling approaches may introduce to the F_{CH_4} data and because the relationship between environmental drivers and whole-ecosystem CH_4 fluxes has yet to be established.

The relationship between NEE and environmental drivers is largely well established, and to fill the gaps in half-hourly NEE, we used the Mitscherlich model (e.g., Aubinet et al., 2001; Reichstein et al., 2012):

$$\text{NEE} = -(\beta_M + \gamma_M) \left(1 - \exp\left(\frac{-\alpha_M \text{PPFD}}{\beta_M + \gamma_M}\right) \right) + \gamma_M, \quad (2)$$

where α_M is the initial slope of the light response curve, β_M is the gross ecosystem productivity (GEP) at light saturation, and γ_M , the intercept parameter at PPFD = $0 \mu\text{mol}\cdot\text{m}^{-2}\cdot\text{s}^{-1}$, represents ecosystem respiration (RE). We chose the Mitscherlich model because it results in realistic values of β_M that can be used study its variability (Reichstein et al., 2012). Parameters were estimated using least squares regression for observations using 7-day moving windows. GEP was calculated as the difference between the estimated RE and the

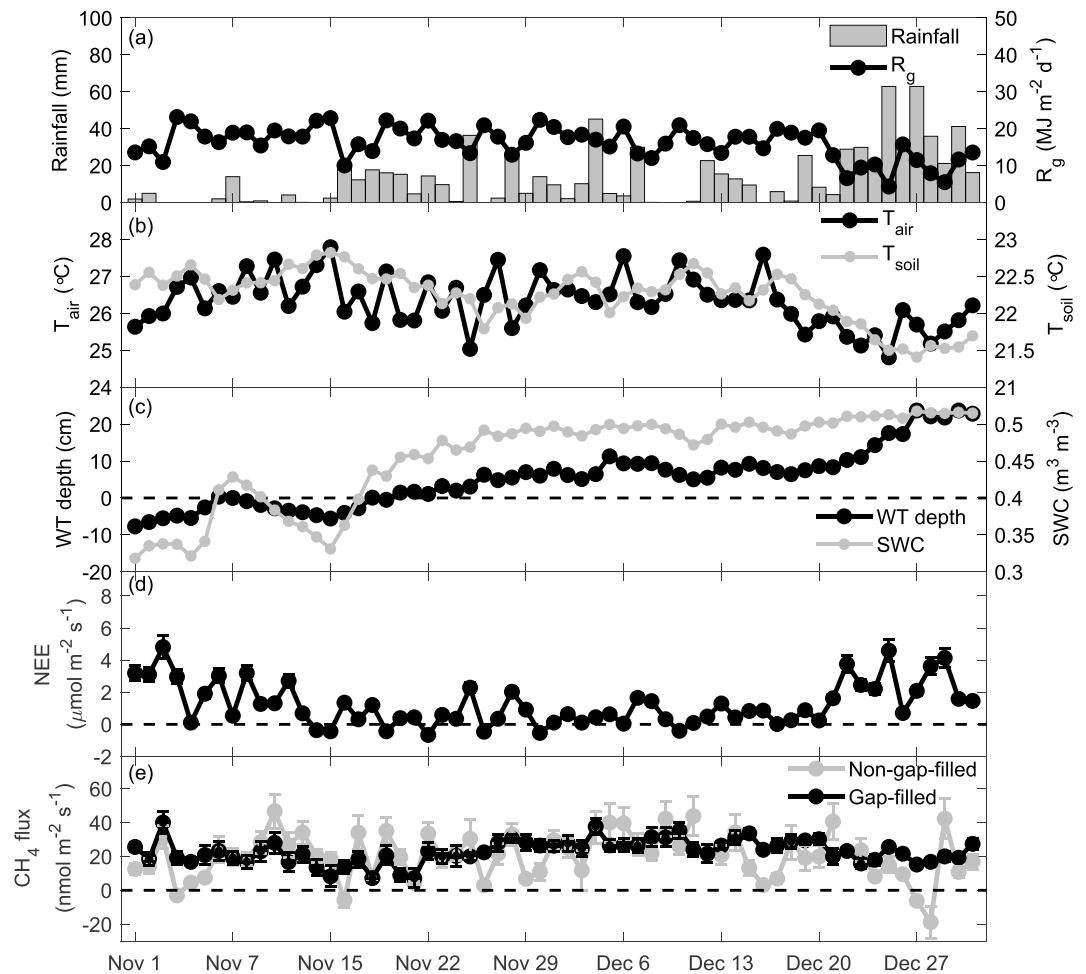


Figure 1. Time series of (a) daily cumulative rainfall, daily mean ($\pm \text{SE}$), (b) air temperature (T_{air}) and soil temperature (T_{s}), (c) water table (WT) depth and soil water content (SWC), (d) net ecosystem CO_2 exchange (NEE), and (e) non-gap-filled and gap-filled methane (CH_4) flux from the November and December 2013 study period in a tropical peat forest ecosystem in Maludam National Park, Malaysian Borneo. For the non-gap-filled CH_4 flux, observed fluxes that passed quality control filters were averaged to arrive at a daily mean, and no observations passed quality control filters on 12 and 22 December. Error bars represent $\pm \text{SE}$.

observed NEE: $\text{GEP} = \text{RE} + \text{NEE}$ using the meteorological convention that negative values indicate ecosystem CO_2 uptake.

2.4. Data Analysis

To understand the relationships between micrometeorological drivers, CO_2 fluxes, and F_{CH_4} , we used least squares regression and identified parsimonious linear models of F_{CH_4} using information criterion techniques via the *dredge* function of the “MuMIn” package in R (Bartoń, 2016). The dredge algorithm creates all possible univariate and multivariate models of a dependent variable (in this case F_{CH_4}) based on independent variables (in this case all micrometeorological measurements and F_{CO_2} measurements described above) and selects the model with the minimum value of the Akaike information criterion (AIC)—the model with the lowest value of the likelihood function by number of model parameters—as the most parsimonious (Akaike, 1974). Given the uncertainties regarding the diurnal time course of F_{CH_4} due to uncertainties regarding the RSSI threshold, we explored models at the daily time scale using the daily sum of F_{CH_4} and daily averages of micrometeorological variables using the small sample size-corrected AIC (AICc) (see Figure S1). Following studies that included carbon dioxide flux as additional explanatory variables for F_{CH_4} (e.g., Christensen et al., 1996), we added NEE, GEP, and RE to the modeling analysis.

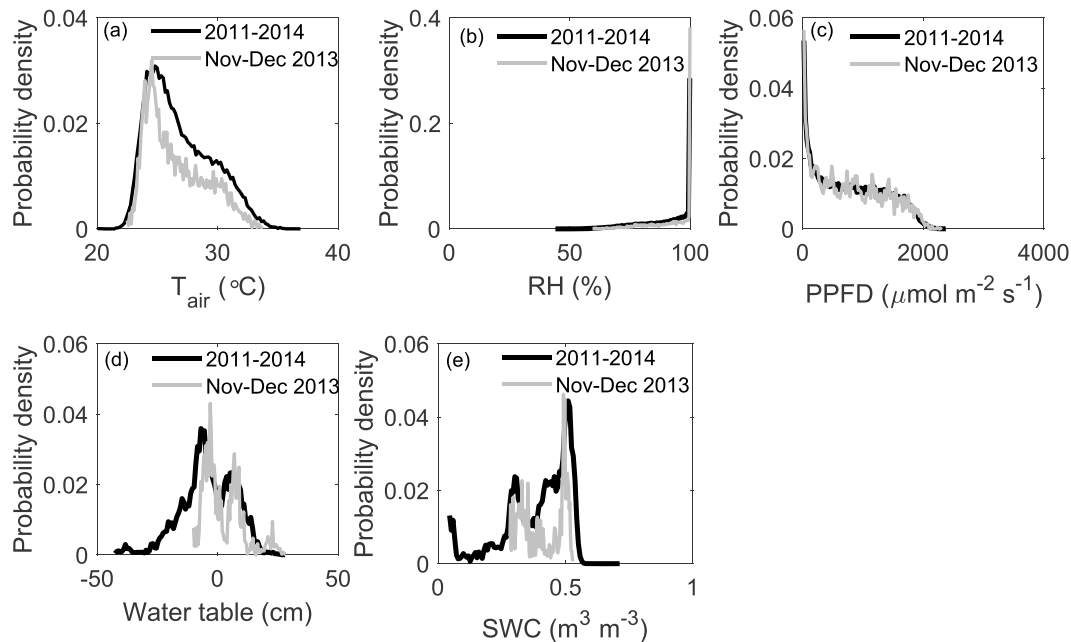


Figure 2. Probability distribution of micrometeorological measurements during the 4-year period (2011–2014) versus the 2-month period (November–December 2013) for (a) air temperature (T_{air}), (b) relative humidity (RH), (c) photosynthetically active photon flux density (PPFD, selecting only daytime values taken to be $>5 \mu\text{mol}\cdot\text{m}^{-2}\cdot\text{s}^{-1}$), (d) water table, and (e) soil water content (SWC).

3. Results

3.1. Micrometeorological Variability and Eddy Covariance Observations

Average T_{air} and R_g decreased from November 2013 (26.5 $^{\circ}\text{C}$; 17.7 $\text{MJ}\cdot\text{m}^{-2}\cdot\text{day}^{-1}$) to December 2013 (26.2 $^{\circ}\text{C}$; 14.6 $\text{MJ}\cdot\text{m}^{-2}\cdot\text{day}^{-1}$), and P increased from 224 to 562 mm/month (Figures 1a and 1b). SWC increased to field capacity—with the exception of a weeklong period of decline in mid-November—as the WT approached and then exceeded the soil surface in late November (Figure 1c). The probability distributions of measurements shows that the T_{air} , RH, incoming PPFD ($>5 \mu\text{mol}\cdot\text{m}^{-2}\cdot\text{s}^{-1}$), WT, and SWC do not vary considerably between the 4-year period of meteorological data availability and the 2-month study period (November–December 2013; Figure 2) excluding dry season periods when the WT was more than 10 cm below the surface. The study period thus encompasses the transition from unsaturated to saturated soil conditions with standing water present throughout December. NEE was positive, indicating CO_2 loss to the atmosphere in early November and at late December (Figure 1d), and was about 0.5 $\mu\text{mol}\cdot\text{m}^{-2}\cdot\text{s}^{-1}$ on average from mid-November until mid-December. Nighttime stability, RSSI filters, and precipitation events resulted in 70% of the available observations being removed from the F_{CH_4} data record to ensure that only high-quality measurements under fully developed turbulence were made. Energy balance closure during the study period was 51%, with the relatively low value attributable in part to advective transport of heat by flowing water at this peatland study site. We did not adjust biogeochemical fluxes as a result of lack of energy balance closure as suggested by Baldocchi (2008).

Wind-rose analyses showed that the wind mainly came from southeast in November and northwest in December (Figure 3a), suggesting a shift in dominant flux source area. As a consequence, we include the sinusoid of wind direction ($\sin(\text{WD})$) in the modeling analysis and perform the modeling analysis for each month in addition to the combined 2-month period to explore if different variables are responsible for F_{CH_4} across time (Figure 1e) and space (Figure 3b).

3.2. CH_4 Flux

Monthly average of gap-filled F_{CH_4} ($\pm\text{SE}$) was higher in December (25.3 \pm 0.6 $\text{nmol}\cdot\text{m}^{-2}\cdot\text{s}^{-1}$) than November (20.3 \pm 0.8 $\text{nmol}\cdot\text{m}^{-2}\cdot\text{s}^{-1}$; $p < 0.05$), but the temporal variability of F_{CH_4} was higher during November than December (Figure 1e). Further, both daytime and nighttime F_{CH_4} were higher in December

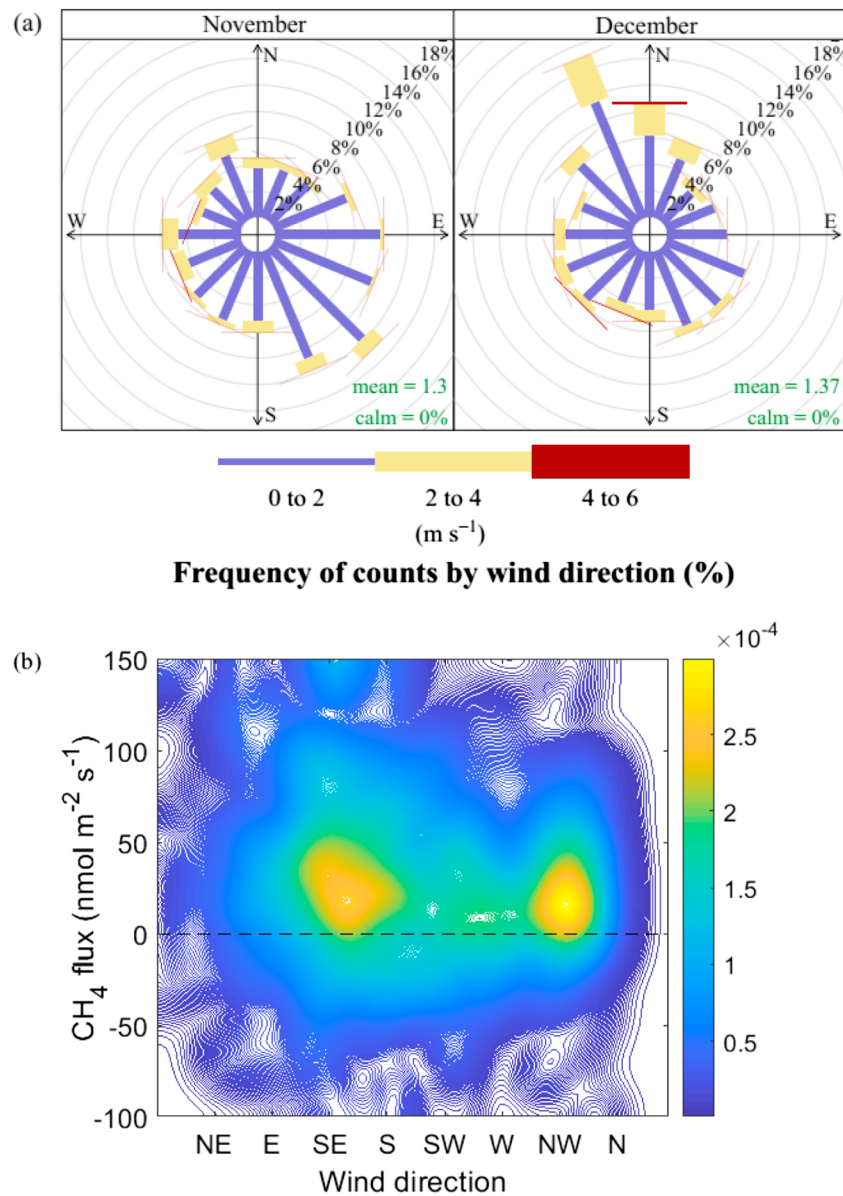


Figure 3. (a) Wind rose indicating the predominant wind direction at the study site during November and December 2013. (b) The relationship between wind direction and CH_4 flux (F_{CH_4}) as represented by a two-dimensional kernel density estimate (“heat map”) for all half-hourly observations.

($30 \pm 1 \text{ nmol}\cdot\text{m}^{-2}\cdot\text{s}^{-1}$; $20 \pm 0.4 \text{ nmol}\cdot\text{m}^{-2}\cdot\text{s}^{-1}$) than November ($27 \pm 1 \text{ nmol}\cdot\text{m}^{-2}\cdot\text{s}^{-1}$; $13 \pm 0.6 \text{ nmol}\cdot\text{m}^{-2}\cdot\text{s}^{-1}$; $p < 0.05$). The half-hourly mean F_{CH_4} exhibited a few peaks in emissions on the order of 45 to 50 $\text{nmol}\cdot\text{m}^{-2}\cdot\text{s}^{-1}$ during the morning hours and began to decline after a peak around 10:00 local standard time (see Figure 4a). Higher F_{CH_4} was observed during the day (07:00–18:30; $29 \pm 1 \text{ nmol}\cdot\text{m}^{-2}\cdot\text{s}^{-1}$) than at night (19:00–06:30; $17 \pm 0.3 \text{ nmol}\cdot\text{m}^{-2}\cdot\text{s}^{-1}$; $p < 0.05$) and a two-dimensional kernel density estimate demonstrates two regions of higher F_{CH_4} that correspond to the shift in WD from the southeast in November to the northwest in December (Figure 3a). NEE during the studied period shows a strong diel pattern with positive nighttime fluxes and maximum uptake of $12.5 \mu\text{mol}\cdot\text{m}^{-2}\cdot\text{s}^{-1}$ at 11:30 hr (Figure 4b).

3.3. Models of Ecosystem-Scale CH_4 Flux

Observations demonstrated little reason to justify nonlinear relationships between driver and response over the observed range of F_{CH_4} and micrometeorological variability (Figure 2); hence, we explore simple multiple linear models of daily F_{CH_4} that have the lowest AICc value for the case of daily measurements. The most

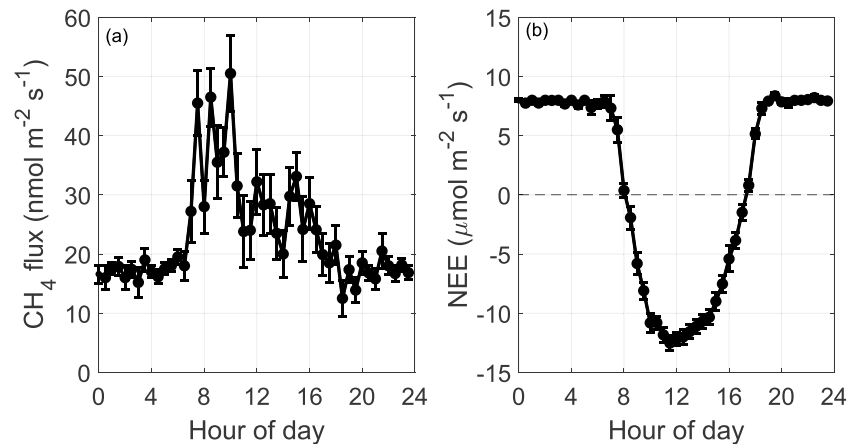


Figure 4. The diurnal pattern of half-hourly gap-filled mean (a) CH₄ flux (F_{CH_4}) and (b) net ecosystem CO₂ exchange during the November–December 2013 measurement period in a tropical peat forest ecosystem in Maludam National Park, Malaysian Borneo. The error bars represent \pm SE.

parsimonious model for the entire measurement period included T_{soil} , SWC, and WT: $F_{CH_4} = 0.254 - 0.012T_{soil} + 0.13$ SWC to 0.001 WT and was able to capture 11% of the variability in daily F_{CH_4} . Including NEE, GEP, and RE did not improve models of F_{CH_4} .

The linear modeling analyses selected different models for November and December, respectively. For November, the model $F_{CH_4} = -0.54 - 0.0034$ RH + 0.0096 T_{air} explains approximately 19% of the variability in daily F_{CH_4} . About 20% of the variance in daily F_{CH_4} can be explained by WT alone in December by $F_{CH_4} = 0.044 - 0.0015$ WT.

Table 1

Mean Daily CH₄ Flux Measured Using the Eddy Covariance Method From Different Ecosystems in North America, Europe, and Asia

Ecosystem	Observation period	CH ₄ flux (g C·m ⁻² ·day ⁻¹)	References
Ponderosa pine, United States	14–19 August, 2007	0.0025	Smeets et al. (2009)
Soybean cropland, United States ^a	May 2011 to May 2012	0.0063	Chu et al. (2014)
Arctic tundra, Russia ^a	20 July 2003 to 19 July 2004	0.0066	Wille et al. (2008)
Aapa mire, Finland	August 1995, May–June 1997, and September–October 1998	0.011	Hargreaves et al. (2001)
Aapa mire, Finland	4–13 June 2008	0.013	Hartley et al. (2015)
Rice paddy, United States ^a	1 March 2012 to 1 March 2013	0.014	Knox et al. (2015)
Pasture, United States ^a	1 March 2012 to 1 March 2013	0.016–0.031	Knox et al. (2015)
Rice fields, Philippines ^a	1 December 2012 to 27 May 2013	0.018	Alberto et al. (2014)
Rice paddy, Taiwan ^a	24 October to 23 November 2006	0.018	Tseng et al. (2010)
Boreal fen, Canada	May–September 2007	0.019	Long et al. (2010)
Tropical peat forest, Malaysia	November–December 2013	0.024	This study
Boreal fen, Finland ^a	March 2005 to February 2006	0.026	Rinne et al. (2007)
Subarctic peatland, Sweden ^a	January 2006 to December 2007	0.056	Jackowicz-Korczyński et al. (2010)
Alpine wetland, China ^a	23 July 2011 to 31 December 2013	0.062	Song et al. (2015)
Subtropical pastures, United States ^a	1 April 2013 to 31 March 2014 and 1 April 2014 to 31 March 2015	0.064	Chamberlain et al. (2017)
Restored old wetland, United States ^a	1 August 2012 to 1 August 2013	0.106	Knox et al. (2015)
Subtropical grass marshland, Taiwan	Mid-August to end of September 2015	0.109	Philipp et al. (2017)
Freshwater marsh, United States ^a	1 March 2012 to 1 March 2013	0.14	Chu et al. (2014)
Restored young wetland, United States ^a	March 2011 to March 2013	0.145	Knox et al. (2015)

Note. Positive values represent net flux from the surface to the atmosphere. Entries in bold compare our CH₄ flux value with other different ecosystems in the world in which the values are sorted in ascending order.

^aSites that include one or more years of quasi-continuous observations.

4. Discussion

Mean eddy covariance-measured F_{CH_4} was on the order of $0.024 \text{ g C-CH}_4\text{m}^{-2}\text{day}^{-1}$ during the November–December 2013 wet season measurement period. These values are of similar magnitude to eddy covariance F_{CH_4} measurements from rice agroecosystems in the Philippines and Taiwan ($\sim 0.018 \text{ g C-CH}_4\text{m}^{-2}\text{day}^{-1}$, Alberto et al., 2014; Tseng et al., 2010; Table 1) measured across an annual period and from boreal fens in Canada (measured during the growing season) and annual measurements from Finland ($\sim 0.019\text{--}0.026 \text{ g C-CH}_4\text{m}^{-2}\text{day}^{-1}$, Long et al., 2010; Rinne et al., 2007). Results demonstrate that the tropical peat rainforest study ecosystem during the wet season is near the mode of F_{CH_4} from other eddy covariance studies from global ecosystems, which ranged from $0.0025 \text{ g C-CH}_4\text{m}^{-2}\text{day}^{-1}$ in a pine plantation (Smeets et al., 2009) to $0.14 \text{ g C-CH}_4\text{m}^{-2}\text{day}^{-1}$ in a freshwater marsh (Chu et al., 2014; Table 1), noting that not all observations, including ours, encompassed an entire year of quasi-continuous eddy covariance measurements.

Modeling analyses revealed relatively poor relationships between micrometeorological variability and daily F_{CH_4} across the entire measurement period, suggesting that above-canopy micrometeorological variables and soil variables measured at a point do not capture whole-ecosystem F_{CH_4} , which may be the result of multiple “hot spot hot moment” dynamics distributed across the flux footprint (Wilson et al., 2009). However, simpler relationships emerged before and after the WT exceeded the surface, coinciding with the transition from November to December (Figure 1c). Atmospheric variable T_{air} was an important model input in November, but the hydrologic variable WT was an important input in December, suggesting a shift in controls over methane efflux from unsaturated to saturated conditions. We note that we cannot exclude a shift in source area from explaining part of the variability in observations and best fit models (Figure 3), but variables related to WD were not identified as contributing to the most parsimonious explanation of CH_4 . Surprisingly, the best fit model for the entire measurement period and for December alone included negative term for WT, suggesting that high WT values may hinder F_{CH_4} by serving as a barrier to diffusion despite an increase in both F_{CH_4} and WT across the measurement period. These results have important implications for ecosystem models by demonstrating the important role of temperature during unsaturated conditions and WT during saturated conditions and further emphasize the critical role of simulating temperature and WT accurately for accurate modeled ecosystem scale F_{CH_4} estimates (Cao et al., 1996; Walter et al., 2001). The importance of WT further emphasizes the importance of ascertaining wetland area, especially tropical wetland area, as a critical present and future uncertainty in the global CH_4 budget (B. Zhang et al., 2017; Z. Zhang et al., 2017).

Combined, measurements demonstrate that CH_4 flux from a tropical peat forest was similar to other managed and natural wetland ecosystems, including those in different climate zones. Results also demonstrate that meteorological variability described F_{CH_4} poorly, in part due to the small range of micrometeorological variables in a tropical peat ecosystem (Figure 2). In brief, F_{CH_4} decreased under dry conditions with decreasing SWC and RH before WT was at or below the surface, then increased once WT rose above the surface in December before decreasing again as WT rose further (Figure 1).

5. Conclusions

Ecosystem-scale observations of F_{CH_4} in an undisturbed tropical peat forest ecosystem in Malaysian Borneo during the wet season demonstrated a CH_4 source on the order of $0.024 \text{ g C-m}^{-2}\text{day}^{-1}$, similar to eddy covariance measurements from rice agroecosystems in Southeast Asia and boreal fens in Finland and Canada (Table 1) and near the mode of F_{CH_4} measurements across global ecosystems using the eddy covariance technique to date, noting that few observations at the annual time scale have been published to date. Modeling results indicate that T_{air} was an important term for describing the variability of F_{CH_4} before standing water emerged, while WT height was important thereafter, but tended to explain only a small part of its variability, on the order of 19% and 20%, respectively. Results do not point to this tropical peat forest as a disproportionate to F_{CH_4} on per unit area basis, but estimates of the area of tropical wetland ecosystems need to be improved, and more ecosystem-scale F_{CH_4} measurements in tropical wetlands need to be made, to better understand their contribution to the global methane budget.

Acknowledgments

This work is supported by both the Sarawak State Government and the Federal Government of Malaysia. P. C. S. acknowledges support from the National Science Foundation Department of Environmental Biology grant 1552976. We would also like to thank Takashi Hirano for his advice and assistance in this study and Rob Payn, Mark Greenwood, and Benjamin Poulter for valuable comments on the manuscript and valuable comments from three referees. The data generated during this study are available at <https://doi.org/10.5281/zenodo.1161966>.

References

- Akaike, H. (1974). A new look at the statistical model identification. *IEEE Transactions on Automatic Control*, 19(6), 716–723. <https://doi.org/10.1109/TAC.1974.1100705>
- Alberto, M. C. R., Wassmann, R., Buresh, R. J., Quilty, J. R., Correa, T. Q., Sandro, J. M., & Centeno, C. A. R. (2014). Measuring methane flux from irrigated rice fields by eddy covariance method using open-path gas analyzer. *Field Crops Research*, 160, 12–21. <https://doi.org/10.1016/j.fcr.2014.02.008>
- Anderson, J. A. R. (1972). *Synoptical key for the identification of the trees of the peat swamp forests of Sarawak*. Sarawak: Forest Department.
- Aubinet, M., Chermanne, B., Vandenhaute, M., Longdoz, B., Yernaux, M., & Laitat, E. (2001). Long term carbon dioxide exchange above a mixed forest in the Belgian Ardennes. *Agricultural and Forest Meteorology*, 108(4), 293–315. [https://doi.org/10.1016/S0168-1923\(01\)00244-1](https://doi.org/10.1016/S0168-1923(01)00244-1)
- Aydin, M., Verhulst, K. R., Saltzman, E. S., Battle, M. O., Montzka, S. A., Blake, D. R., et al. (2011). Recent decreases in fossil-fuel emissions of ethane and methane derived from firm air. *Nature*, 476(7359), 198–201. <http://doi.org/10.1038/nature10352>
- Bartoň, K. (2016). MuMIn: Multi-Model Inference. R package version 1.15.6. Retrieved from <http://cran.r-project.org/package=MuMIn>
- Baldocchi, D. (2008). “Breathing” of the terrestrial biosphere: Lessons learned from a global network of carbon dioxide flux measurement systems. *Australian Journal of Botany*, 56(1), 1–26. <https://doi.org/10.1071/BT07151>
- Bloom, A. A., Lee-Taylor, J., Madronich, S., Messenger, D. J., Palmer, P. I., Reay, D. S., & McLeod, A. R. (2010). Global methane emission estimates from ultraviolet irradiation of terrestrial plant foliage. *New Phytologist*, 187(2), 417–425. <https://doi.org/10.1111/j.1469-8137.2010.03259.x>
- Bousquet, P., Ringeval, B., Pison, I., Dlugokencky, E. J., Brunke, E. G., Carouge, C., et al. (2011). Source attribution of the changes in atmospheric methane for 2006–2008. *Atmospheric Chemistry and Physics*, 11(8), 3689–3700. <https://doi.org/10.5194/acp-11-3689-2011>
- Campbell, G. S., & Norman, J. M. (2012). *An introduction to environmental biophysics*. New York: Springer Science & Business Media.
- Cao, M., Marshall, S., & Gregson, K. (1996). Global carbon exchange and methane emissions from natural wetlands: Application of a process-based model. *Journal of Geophysical Research*, 101(D9), 14,399–14,414. <https://doi.org/10.1029/96JD00219>
- Chamberlain, S. D., Groffman, P. M., Boughton, E. H., Gomez-Casanovas, N., DeLucia, E. H., Bernacchi, C. J., & Sparks, J. P. (2017). The impact of water management practices on subtropical pasture methane emissions and ecosystem service payments. *Ecological Applications*, 27(4), 1199–1209. <https://doi.org/10.1002/eap.1514>
- Christensen, T. R., Prentice, I. C., Kaplan, J., Haxeltine, A., & Sitch, S. (1996). Methane flux from northern wetlands and tundra. *Tellus Series B: Chemical and Physical Meteorology*, 48(5), 652–661. <https://doi.org/10.3402/tellusb.v48i5.15938>
- Chu, H., Chen, J., Gottgens, J. F., Ouyang, Z., John, R., Czajkowski, K., & Becker, R. (2014). Net ecosystem methane and carbon dioxide exchanges in a Lake Erie coastal marsh and a nearby cropland. *Journal of Geophysical Research: Biogeosciences*, 119, 722–740. <https://doi.org/10.1002/2013JG002520>
- Dargie, G. C., Lewis, S. L., Lawson, I. T., Mitchard, E. T. A., Page, S. E., Bocko, Y. E., & Ifo, S. A. (2017). Age, extent and carbon storage of the Central Congo Basin peatland complex. *Nature*, 542(7639), 86–90. <https://doi.org/10.1038/nature>
- Denman, K. L., Brasseur, G., Chidthaisong, A., Ciais, P., Cox, P. M., Dickinson, R. E., et al. (2007). Couplings between changes in the climate system and biogeochemistry. In S. Solomon & D. Qin (Eds.), *Climate change 2007: The physical science basis. Contribution of Working Group I to the Fourth Assessment Report of the Intergovernmental Panel on Climate Change* (pp. 500–587). Cambridge, UK, and New York: Cambridge University Press.
- Dlugokencky, E. (2017). NOAA/ESRL. Retrieved from www.esrl.noaa.gov/gmd/ccgg/trends_ch4/
- Gu, L., Massman, W. J., Leuning, R., Pallardy, S. G., Meyers, T., Hanson, P. J., et al. (2012). The fundamental equation of eddy covariance and its application in flux measurements. *Agricultural and Forest Meteorology*, 152(1), 135–148. <https://doi.org/10.1016/j.agrformet.2011.09.014>
- Hargreaves, K. J., Fowler, D., Pitcairn, C. E. R., & Aurela, M. (2001). Annual methane emission from Finnish mires estimated from eddy covariance campaign measurements. *Theoretical and Applied Climatology*, 70(1–4), 203–213. <https://doi.org/10.1007/s007040170015>
- Hartley, I. P., Hill, T. C., Wade, T. J., Clement, R. J., Moncrieff, J. B., Prieto-Blanco, A., et al. (2015). Quantifying landscape-level methane fluxes in subarctic Finland using a multiscale approach. *Global Change Biology*, 21(10), 3712–3725. <https://doi.org/10.1111/gcb.12975>
- Hausmann, P., Sussmann, R., & Smale, D. (2016). Contribution of oil and natural gas production to renewed increase in atmospheric methane (2007–2014): Top-down estimate from ethane and methane column observations. *Atmospheric Chemistry and Physics*, 16(5), 3227–3244. <http://doi.org/10.5194/acp-16-3227-2016>
- Hayek, M. N., Wehr, R., Longo, M., Hutyrá, L. R., Wiedemann, K., Munger, J. W., et al. (2018). A novel correction for biases in forest eddy covariance carbon balance. *Agricultural and Forest Meteorology*, 250–251, 90–101. <https://doi.org/10.1016/J.AGRFORMET.2017.12.186>
- Helmig, D., Rossabi, S., Hueber, J., Tans, P., Montzka, S. A., Masarie, K., et al. (2016). Reversal of global atmospheric ethane and propane trends largely due to US oil and natural gas production. *Nature Geoscience*, 9(7), 490–495. <http://doi.org/10.1038/ngeo2721>
- Jackowicz-Korczyński, M., Christensen, T. R., Bäckstrand, K., Crill, P., Friborg, T., Mastepanov, M., & Ström, L. (2010). Annual cycle of methane emission from a subarctic peatland. *Journal of Geophysical Research*, 115, G02009. <https://doi.org/10.1029/2008JG000913>
- Jocher, G., De Simon, G., Hörnlund, T., Linder, S., Lundmark, T., Marshall, J., et al. (2017). Apparent winter CO₂ uptake by a boreal forest due to decoupling. *Agricultural and Forest Meteorology*, 232, 23–34. <https://doi.org/10.1016/J.AGRFORMET.2016.08.002>
- Kai, F. M., Tyler, S. C., Randerson, J. T., & Blake, D. R. (2011). Reduced methane growth rate explained by decreased Northern Hemisphere microbial sources. *Nature*, 476(7359), 194–197. <http://doi.org/10.1038/nature10259>
- Keppler, F., Hamilton, J. T., Bra, M., & Rockmann, T. (2006). Methane emissions from terrestrial plants under aerobic conditions. *Nature*, 439(7073), 187–191. <https://doi.org/10.1038/nature04420>
- Kirschke, S., Bousquet, P., Ciais, P., Saunoy, M., Canadell, J. G., Dlugokencky, E. J., et al. (2013). Three decades of global methane sources and sinks. *Nature Geoscience*, 6(10), 813–823. <https://doi.org/10.1038/ngeo1955>
- Knox, S. H., Sturtevant, C., Matthes, J. H., Koteen, L., Verfaillie, J., & Baldocchi, D. (2015). Agricultural peatland restoration: Effects of land-use change on greenhouse gas (CO₂ and CH₄) fluxes in the Sacramento-San Joaquin Delta. *Global Change Biology*, 21(2), 750–765. <https://doi.org/10.1111/gcb.12745>
- Levin, I., Veidt, C., Vaughn, B. H., Brailsford, G., Bromley, T., Heinz, R., et al. (2012). No inter-hemispheric δ¹³C₄ trend observed. *Nature*, 486(7404), E3–E4. <http://doi.org/10.1038/nature11175>
- Long, K. D., Flanagan, L. B., & Cai, T. (2010). Diurnal and seasonal variation in methane emissions in a northern Canadian peatland measured by eddy covariance. *Global Change Biology*, 16(9), 2420–2435. <https://doi.org/10.1111/j.1365-2486.2009.02083.x>
- Massman, W. J. (2000). A simple method for estimating frequency response corrections for eddy covariance systems. *Agricultural and Forest Meteorology*, 104(3), 185–198. [https://doi.org/10.1016/S0168-1923\(00\)00164-7](https://doi.org/10.1016/S0168-1923(00)00164-7)
- McDermitt, D., Burba, G., Xu, L., Anderson, T., Komisarov, A., Riensche, B., et al. (2011). A new low-power, open-path instrument for measuring methane flux by eddy covariance. *Applied Physics B: Lasers and Optics*, 102(2), 391–405. <https://doi.org/10.1007/s00340-010-4307-0>
- McLeod, A. R., Fry, S. C., Loake, G. J., Messenger, D. J., Reay, D. S., Smith, K. A., & Yun, B. W. (2008). Ultraviolet radiation drives methane emissions from terrestrial plant pectins. *New Phytologist*, 180(1), 124–132. <https://doi.org/10.1111/j.1469-8137.2008.02571.x>

- Mhyre, G., Shindell, D., Bréon, F. M., Collins, W., Fuglestedt, J., Huang, J., et al. (2013). Anthropogenic and natural radiative forcing. *Climate Change*, 423, 658–740. <https://doi.org/10.1017/CBO9781107415324.018>
- Nisbet, E. G., Dlugokencky, E. J., Manning, M. R., Lowry, D., Fisher, R. E., France, J. L., et al. (2016). Rising atmospheric methane: 2007–2014 growth and isotopic shift. *Global Biogeochemical Cycles*, 30, 1356–1370. <https://doi.org/10.1002/2016GB005406>
- Novick, K. A., Stoy, P. C., Katul, G. G., Ellsworth, D. S., Siqueira, M. B. S., Juang, J., & Oren, R. (2004). Carbon dioxide and water vapor exchange in a warm temperate grassland. *Oecologia*, 138(2), 259–274. <https://doi.org/10.1007/s00442-003-1388-z>
- Pangala, S. R., Enrich-Prast, A., Basso, L. S., Peixoto, R. B., Bastviken, D., Hornibrook, E. R., et al. (2017). Large emissions from floodplain trees close the Amazon methane budget. *Nature*, 552(7684), 230–234. <https://doi.org/10.1038/nature24639>
- Pangala, S. R., Moore, S., Hornibrook, E. R., & Gauci, V. (2013). Trees are major conduits for methane egress from tropical forested wetlands. *New Phytologist*, 197(2), 524–531. <https://doi.org/10.1111/nph.12031>
- Pandey, S., Houweling, S., Krol, M., Aben, I., Monteil, G., Nechita-Banda, N., et al. (2017). Enhanced methane emissions from tropical wetlands during the 2011 La Niña. *Scientific Reports*, 7, 45759. <https://doi.org/10.1038/srep45759>
- Philipp, K., Juang, J. Y., Deventer, M. J., & Klemm, O. (2017). Methane emissions from a subtropical grass marshland, northern Taiwan. *Wetlands*, 37(6), 1145–1157. <https://doi.org/10.1007/s13157-017-0947-8>
- Pison, I., Ringeval, B., Bousquet, P., Prigent, C., & Papa, F. (2013). Stable atmospheric methane in the 2000s: Key-role of emissions from natural wetlands. *Atmospheric Chemistry and Physics*, 13(23), 11,609–11,623. <https://doi.org/10.5194/acp-13-11609-2013>
- Pitz, S., & Megonigal, J. P. (2017). Temperate forest methane sink diminished by tree emissions. *New Phytologist*, 214(4), 1432–1439. <https://doi.org/10.1111/nph.14559>
- Reichstein, M., Falge, E., Baldocchi, D., Papale, D., Aubinet, M., Berbigier, P., et al. (2005). On the separation of net ecosystem exchange into assimilation and ecosystem respiration: Review and improved algorithm. *Global Change Biology*, 11(9), 1424–1439. <https://doi.org/10.1111/j.1365-2486.2005.001002.x>
- Reichstein, M., & Moffat, A. M. (2014). REddyProc: Data processing and plotting utilities of (half-) hourly eddy-covariance measurements. R package version 0.6–0/r9.
- Reichstein, M., Stoy, P. C., Desai, A. R., Lasslop, G., & Richardson, A. D. (2012). Partitioning of net fluxes. In *Eddy covariance* (pp. 263–289). Netherlands: Springer.
- Rice, A. L., Butenhoff, C. L., Teama, D. G., Röger, F. H., Khalil, M. A. K., & Rasmussen, R. A. (2016). Atmospheric methane isotopic record favors fossil sources flat in 1980s and 1990s with recent increase. *Proceedings of the National Academy of Sciences*, 113(39), 10,791–10,796. <http://doi.org/10.1073/pnas.1522923113>
- Rinne, J., Riutta, T., Pihlatie, M., Aurela, M., Haapanala, S., Tuovinen, J. P., et al. (2007). Annual cycle of methane emission from a boreal fen measured by the eddy covariance technique. *Tellus Series B: Chemical and Physical Meteorology*, 59(3), 449–457. <https://doi.org/10.1111/j.1600-0889.2007.00261.x>
- Saunio, M., Bousquet, P., Poulter, B., Peregon, A., Ciais, P., Canadell, J. G., et al. (2016). The global methane budget 2000–2012. *Earth System Science Data*, 8(2), 697–751. <http://doi.org/10.5194/essd-8-697-2016>
- Saunio, M., Jackson, R. B., Bousquet, P., Poulter, B., & Canadell, J. G. (2016). The growing role of methane in anthropogenic climate change. *Environmental Research Letters*, 11(12), 120207. <https://doi.org/10.1088/1748-9326/11/12/120207>
- Schaefer, H., Fletcher, S. E. M., Veidt, C., Lassey, K. R., Brailsford, G. W., Bromley, T. M., et al. (2016). A 21st-century shift from fossil-fuel to biogenic methane emissions indicated by ¹³CH₄. *Science*, 352(6281), 80–84. <https://doi.org/10.1126/science.aad2705>
- Schwietzke, S., Sherwood, O. A., Bruhwiler, L. M. P., Miller, J. B., Etiope, G., Dlugokencky, E. J., et al. (2016). Upward revision of global fossil fuel methane emissions based on isotope database. *Nature*, 538(7623), 88–91. <https://doi.org/10.1038/nature19797>
- Shindell, D., Kuylenstierna, J. C. I., Vignati, E., van Dingenen, R., Amann, M., Klimont, Z., et al. (2012). Simultaneously mitigating near-term climate change and improving human health and food security. *Science*, 335(6065), 183–189. <https://doi.org/10.1126/science.1210026>
- Simpson, I. J., Andersen, M. P. S., Meinardi, S., Bruhwiler, L., Blake, N. J., Helmig, D., et al. (2012). Long-term decline of global atmospheric ethane concentrations and implications for methane. *Nature*, 488(7412), 490–494. <https://doi.org/10.1038/nature11342>
- Smeets, C. J. P. P., Holzinger, R., Vigano, I., Goldstein, A. H., & Röckmann, T. (2009). Eddy covariance methane measurements at a Ponderosa pine plantation in California. *Atmospheric Chemistry and Physics Discussions*, 9(1), 5201–5229. <https://doi.org/10.5194/acpd-9-5201-2009>
- Song, W., Wang, H., Wang, G., Chen, L., Jin, Z., Zhuang, Q., & He, J. S. (2015). Methane emissions from an alpine wetland on the Tibetan Plateau: Neglected but vital contribution of the nongrowing season. *Journal of Geophysical Research: Biogeosciences*, 120, 1475–1490. <https://doi.org/10.1002/2015JG003043>
- Tseng, K. H., Tsai, J. L., Alagesan, A., Tsuang, B. J., Yao, M. H., & Kuo, P. H. (2010). Determination of methane and carbon dioxide fluxes during the rice maturity period in Taiwan by combining profile and eddy covariance measurements. *Agricultural and Forest Meteorology*, 150(6), 852–859. <https://doi.org/10.1016/j.agrformet.2010.04.007>
- Turner, A. J., Frankenberg, C., Wennberg, P. O., & Jacob, D. J. (2017). Ambiguity in the causes for decadal trends in atmospheric methane and hydroxyl. *Proceedings of the National Academy of Sciences of the United States of America*, 114(21), 5367–5372. <https://doi.org/10.1073/pnas.1616020114>
- Walter, B. P., Heimann, M., & Matthews, E. (2001). Modeling modern methane emissions from natural wetlands: 1. Model description and results. *Journal of Geophysical Research*, 106(D24), 34,189–34,206. <https://doi.org/10.1029/2001JD900165>
- Webb, E. K., Pearman, G. I., & Leuning, R. (1980). Correction of flux measurements for density effects due to heat and water vapour transfer. *Quarterly Journal of the Royal Meteorological Society*, 106(447), 85–100. <https://doi.org/10.1002/qj.49710644707>
- Wille, C., Kutzbach, L., Sachs, T., Wagner, D., & Pfeiffer, E. M. (2008). Methane emission from Siberian arctic polygonal tundra: Eddy covariance measurements and modeling. *Global Change Biology*, 14(6), 1395–1408. <https://doi.org/10.1111/j.1365-2486.2008.01586.x>
- Wilson, D., Alm, J., Laine, J., Byrne, K. A., Farrell, E. P., & Tuittila, E. S. (2009). Rewetting of cutaway peatlands: Are we re-creating hot spots of methane emissions? *Restoration Ecology*, 17(6), 796–806. <https://doi.org/10.1111/j.1526-100X.2008.00416.x>
- Worden, J. R., Bloom, A. A., Pandey, S., Jiang, Z., Worden, H. M., Walker, T. W., et al. (2017). Reduced biomass burning emissions reconcile conflicting estimates of the post-2006 atmospheric methane budget. *Nature Communications*, 8(1), 2227. <http://doi.org/10.1038/s41467-017-02246-0>
- Zhang, B., Tian, H., Lu, C., Chen, G., Pan, S., Anderson, C., & Poulter, B. (2017). Methane emissions from global wetlands: An assessment of the uncertainty associated with various wetland extent data sets. *Atmospheric Environment*, 165, 310–321. <https://doi.org/10.1016/j.atmosenv.2017.07.001>
- Zhang, Z., Zimmermann, N. E., Stenke, A., Li, X., Hodson, E. L., Zhu, G., et al. (2017). Emerging role of wetland methane emissions in driving 21st century climate change. *Proceedings of the National Academy of Sciences of the United States of America*, 114(36), 9647–9652. <https://doi.org/10.1073/pnas.1618765114>